

Special Issue:

Special Issue on COVID-19 Aerosol
Drivers, Impacts and Mitigation (XI)

Surprising Changes in Aerosol Loading over India amid COVID-19 Lockdown

Satyendra K. Pandey*, V. Vinoj

School of Earth, Ocean and Climate Science Indian Institute of Technology Bhubaneswar, Jatni – 752050, Odisha, India

ABSTRACT

Using ground-based and satellite observation along with aerosol reanalysis products, we show a widespread reduction in aerosol loading over the Indian subcontinent during the COVID-19 (CORonaVirus Disease 2019) lockdown. The pre-lockdown and lockdown period considered in the present study is 20th February–20th March 2020 and 24th March–22nd April 2020. In terms of aerosol optical depth (AOD), loading has reduced up to 40% over the most populated region of India. However, the central part of India shows an unexpected increase (~+20%) in AOD. A simultaneous increase (decrease) in mid-tropospheric relative humidity (wind speed (WS) at 850 hPa) by $+85 \pm 6.0\%$ ($-12 \pm 3.9\%$) occurred during the lockdown. It is found that on a daily scale, the mean AOD is positively (negatively) correlated with mid-tropospheric RH (WS) with a statistically significant linear correlation coefficient of 0.53 (–0.43). An increase (decrease) in RH (WS) of 20% (1 m s^{-1}) was observed to increase AOD by 0.10 (0.04). Thus, we hypothesize that during the lockdown, the increased AOD over central India was due to increased atmospheric moisture coupled with stagnant circulation condition.

Keywords: COVID-19, Lockdown, Aerosols, Air pollution, Humidity

1 INTRODUCTION

The World Health Organization (WHO) declared a global health emergency in January 2020 due to the newly found contagious coronavirus disease named COVID-19. The virus (SARS-CoV-2, Severe Acute Respiratory Syndrome–CoronaVirus-2) responsible for it is of zoonotic origin and was first reported in Wuhan, China, during late December 2019 (Huang *et al.*, 2020; Zhou *et al.*, 2020). Globally, the total death toll of 484,249 and the number of reported cases reached 9,473,214 (as of 26th June 2020) (WHO, 2020). This pandemic caused an unprecedented response from the countries leading to a complete or partial shutdown of human activities. Governments in the South Asian regions, including India, also announced nationwide lockdown in the late March 2020, confining residents to their home except essential services.


Studies across the globe reported a significant change in various environmental and ecological indicators due to limited human activity. Whereas lockdown improved air and water quality (Chauhan and Singh, 2020; Paital, 2020; Yunus *et al.*, 2020), reduced CO₂ (carbon dioxide) level (Le Quéré *et al.*, 2020), cleaned beaches, bloomed wildlife, it adversely affected waste recycling (Zambrano-Monserrate *et al.*, 2020). Primary air-pollutants like NO₂ (nitrogen dioxide), SO₂ (sulfur dioxide), CO (carbon monoxide), particulate pollution (PM_{2.5} and PM₁₀; particulate matter of diameter less than 2.5 μm and 10 μm), and aerosol have plummeted around the world (Berman and Ebisu, 2020; Lal *et al.*, 2020; Muhammad *et al.*, 2020; Shi and Brasseur, 2020; Sicard *et al.*, 2020). Majority of the studies related to lockdown induced reduction in air-pollutant focussed over China. Studies over China invariably show a reduction in CO, NO₂, and PM_{2.5} concentrations (Bao and Zhang, 2020; Bauwens *et al.*, 2020; Filonchik *et al.*, 2020; Shi and Brasseur, 2020; Wang and Su, 2020). Indian region also shows a significant reduction in these air-pollutants (Gautam, 2020; Jain and Sharma, 2020; Lokhandwala and Gautam, 2020; Navinya *et al.*, 2020b; Sharma *et al.*

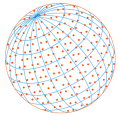
OPEN ACCESS 

Received: July 30, 2020
Revised: October 12, 2020
Accepted: November 11, 2020

* **Corresponding Author:**
sp25@iitbbs.ac.in

Publisher:
Taiwan Association for Aerosol
Research
ISSN: 1680-8584 print
ISSN: 2071-1409 online

 **Copyright:** The Author(s).
This is an open access article
distributed under the terms of the
[Creative Commons Attribution
License \(CC BY 4.0\)](https://creativecommons.org/licenses/by/4.0/), which permits
unrestricted use, distribution, and
reproduction in any medium,
provided the original author and
source are cited.



al., 2020). For example, the concentration of PM_{2.5} and PM₁₀ at the surface level has reduced by 50% over Delhi (Mahato *et al.*, 2020).

Despite an overwhelming reduction of major air-pollutants, several regions show an increase in surface PM_{2.5} concentration, O₃ (ozone) level, aerosol loading, and hazy sky (Le *et al.*, 2020; Li *et al.*, 2020; Sicard *et al.*, 2020). For example, a recent study has shown an enhanced pollution episode over Northern China, despite the cutting of significant emissions, attributable to aerosol-chemistry-meteorology interaction (Le *et al.*, 2020). During the lockdown period, over the Yangtze River Delta, residual pollutants were still high, the majority of which contributed from the industry, residential sectors, and long-range transport (Li *et al.*, 2020). Also, over the Indian region, it is found that using space-borne observation of aerosol optical depth was non-uniform (Gautam, 2020). The aerosol loading over the Indian region is not only affected by anthropogenic pollution, but natural aerosol (such as desert dust, sea-salt) and biomass burning also contribute significantly (Vinoj *et al.*, 2010; Pandey *et al.*, 2016; Tiwari *et al.*, 2016; Yang *et al.*, 2019; Mukherjee and Vinoj, 2020). Therefore, variation in the amount of atmospheric aerosol may not necessarily follow surface pollutants. However, such large-scale changes in aerosol characteristics over one of the world's most polluted regions have the potential to modulate the radiation budget through direct, indirect, and semi-direct radiative effects and regional climate (Satheesh and Ramanathan, 2000; Vinoj and Satheesh, 2004; Pandey *et al.*, 2020). The present study focuses explicitly on the changes in aerosol loading during the lockdown. Here, we attempt to explain the observed spatio-temporal variability of aerosol over India during the lockdown, using ground-based and space-borne aerosol observations along with aerosol and meteorological reanalysis data.

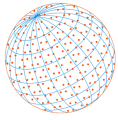
2 DATA AND METHODS

2.1 MODIS

The Moderate Resolution Imaging Spectroradiometer (MODIS) is a multichannel imager onboard NASA's Terra (EOS AM, since 1999) and Aqua (EOS PM, since 2000) satellites that provide high-quality remote sensing observations of land, ocean, and atmosphere. It consists of 36 bands in the wavelength range of 0.4 μm to 14.4 μm that acquires data at varying spatial resolutions (250 m, 500 m, and 1 km). Primary products used in the present study are aerosol, cloud parameters, and atmospheric moisture. We used daily observations of aerosol optical depth (AOD) from both MODIS Terra (MOD08_D3) and Aqua (MYD08_D3) collection 6.1 Level 3 product for the period from 2003 to 2020 (Levy *et al.*, 2013; Wei *et al.*, 2019a, b). In the present study, we have used a combined Dark Target (DT) Deep Blue (DB) AOD at 550 nm, which takes advantage of both dark target (Levy *et al.*, 2013) and deep blue (Hsu *et al.*, 2013) algorithms. Past study over the Indian region has shown that the combined product is in better agreement with ground-based observations than the individual dark target and deep blue retrievals (Mhawish *et al.*, 2017) and covers a larger area. The DTDB is retrieved based on the Normalized Difference Vegetation Index (NDVI) of the underlying surface, if NDVI > 0.3, use DT retrievals, and if NDVI < 0.2, use DB retrievals and if $0.2 \leq \text{NDVI} \leq 0.3$ it uses the average of DT and DB provided it satisfy quality assurance criteria.

2.2 AERONET

Ground-based spectral AOD measurement was obtained from NASA's AERONET (AErosol RObotic NETwork) sites situated over the South Asian region. The AERONET is a global network that provides high-quality observation of aerosol properties, optical depth, angstrom exponent, single scattering albedo, etc., at high temporal resolution (Holben *et al.*, 1998). In the present study, level-1.5 version-3.0 cloud screen daily AOD (at 550 nm) observations were used. The retrieval algorithm has gone through substantial improvement in version 3, as compared to version 2. It includes a new polarized radiative transfer code and fully automated near-real-time quality assurance (Giles *et al.*, 2019; Sinyuk *et al.*, 2020). AOD is the most fundamental parameter retrieved using direct sun algorithm and has an uncertainty of less than ± 0.01 (for $\lambda > 440$ nm) and less than ± 0.02 (for $\lambda < 440$ nm). Six sites (see Fig. 2(a)) were selected based on the criteria of having the AOD measurement during the lockdown period.



2.3 MERRA2

The Modern-Era Retrospective Analysis for Research and Application - version 2, is a state-of-the-art reanalysis product. It uses NASA's Goddard Earth Observing System (GEOS-5) atmospheric general circulation model and the assimilation of space-borne and ground-based observations of various meteorological parameters (Gelaro *et al.*, 2017). The spatial resolution of the model is $0.5^\circ \times 0.625^\circ$ and 72 hybrid-eta levels from the surface up to 0.01 hPa. It simulates five aerosol species (i.e., dust, sea salt, black carbon, organic carbon, and sulfate) using GOCART (Goddard Chemistry Aerosol Radiation and Transport) module. Aerosol reanalysis products benefit from the assimilation of bias-corrected and cloud screened aerosol optical depth observed from space-borne sensors (MODIS, AVHRR, and MISR-Multiangle Imaging SpectroRadiometer) and ground-based (i.e., AERONET) (Buchard *et al.*, 2017; Randles *et al.*, 2017). Aerosol reanalysis products have been widely used in past studies (McCoy *et al.*, 2017; Pandey *et al.*, 2017; Kramer *et al.*, 2018; Navinya *et al.*, 2020a).

2.4 ERA5

Meteorological reanalysis data used in the present study were obtained from the European Center for Medium-Range Weather Forecasts (ECMWF). Recently released, the fifth generation of ECFWF reanalysis, ERA5 (Hersbach *et al.*, 2019), has added advantage compared to its predecessor reanalysis ERA-Interim (Dee *et al.*, 2011). It provides data at a higher spatial and temporal resolution, a better global balance of precipitation and evaporation, improved soil moisture, more consistent sea surface temperature, and sea ice. Moreover, the troposphere is much more improved. The spatial resolution of the data is 31 km ($\sim 0.25^\circ$) and 137 vertical levels from the surface to 0.01 hPa (~ 80 km). A large number of atmospheric, land, and oceanic parameters are available at a frequency of 1 hour. In the present study, we used wind speed, relative humidity, and specific humidity data.

3 RESULTS AND DISCUSSION

3.1 Change in Aerosol Loading during the Lockdown

In order to quantify the impact of lockdown on the aerosol loading, we have chosen two periods; pre-lockdown (20th February–20th March 2020) and during lockdown (24th March–22nd April 2020). The difference between these two periods provides the contribution due to lockdown, if any, after consideration for any climatological features. This is because, apart from the changes due to lockdown, there are inherent seasonal differences in the aerosol loading in these two selected periods. Therefore, we first discuss the climatological difference between these periods. Climatologically, the period considered as lockdown to the pre-lockdown period has significantly higher aerosol loading over South Asia (Fig. 1(c)). Especially peninsular India, the western part, east coast, and northern Bay of Bengal experience high aerosol loading. However, north India, especially the Indo Gangetic Plain (IGP), shows a slight decrease that may be a result of enhanced wind speed as a transition from winter to summer. During the year 2020, this transition shows a prevalent reduction of AOD over northern India, including Pakistan and Bangladesh, which otherwise would have increased. South India also shows a significant decrease in AOD. However, despite pan-India lockdown, mid peninsular India shows higher value compared to the pre-lockdown period. In the year 2020, aerosol loading was exceptionally higher compared to climatology (see Fig. 1(g)). Notably, the AOD anomalies were predominantly positive, except few regions, where slightly negative anomalies were observed. However, during the lockdown period over Northern and Southern India, Pakistan and Bangladesh experienced a significant reduction in AOD compared to climatology. However, anomalies over the mid-peninsular region remain positive. Therefore, Indian states, Maharastra, Telangana, Chattisgarh, and Odisha, still experienced higher aerosol loading. The difference between the two anomalies (Figs. 1(g) and 1(h)) gives the exact magnitude of changes due to lockdown, taking into consideration the climatology. Prevalent reduction in aerosol loading over the larger part of the Indian subcontinent is the result of reduced anthropogenic emissions of primary aerosol and precursor gases.

Analysis with MODIS onboard Aqua (afternoon satellite) and MERRA2 reanalysis data shows the spatial pattern of changes is similar to Terra (Figs. 2(a)–2(c)). For detailed analysis, the study

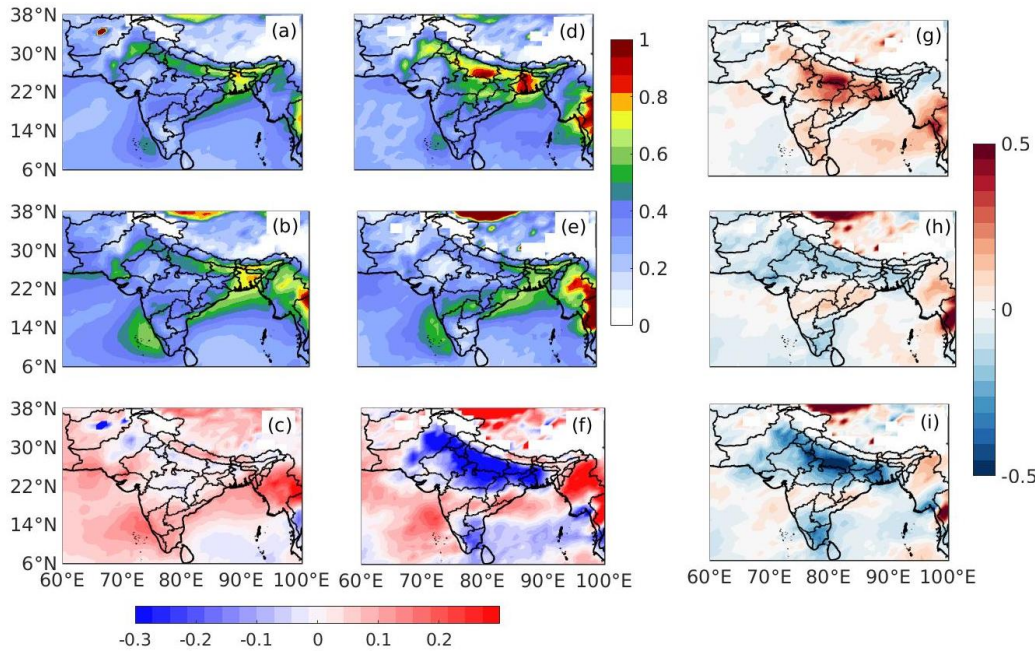
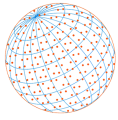


Fig. 1. Aerosol optical depth during (a) pre-lockdown period (b) the lockdown and (c) difference (lockdown minus pre-lockdown) based on their climatology and same analysis for similar periods for the year 2020 (d-e and f)). (g-i) are the difference between column 2 and 1. The data source is MODIS Terra.

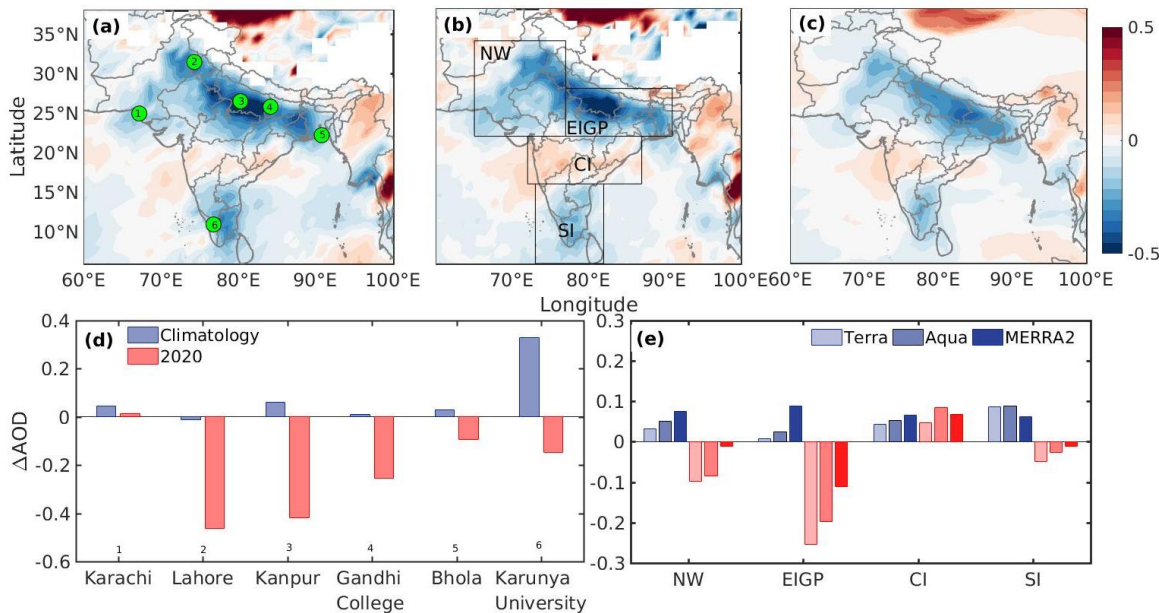
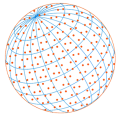


Fig. 2. Spatial pattern of changes in extinction aerosol optical depth using (a) MODIS-Terra, (b) MODIS-Aqua and (c) MERRA2 due to lockdown. The difference in AOD corresponding to lockdown and pre-lockdown period using (d) AERONET observation, and (e) Terra, Aqua, and MERRA2. Green circles are the location of AERONET sites. Blue bar represents climatology (2003–2019) and red for the year 2020.

region was divided into four regions, namely; North West (NW), East IGP (EIGP), Central India (CI), and Southern India (SI) (Fig. 2(b)). The time series of daily averaged AOD over these regions, except CI, shows an abrupt decrease in AOD values following the day of lockdown announcement (Fig. S1). Climatologically, average AOD for the period corresponding to lockdown has higher AOD values across the subcontinent. AOD over NE, EIGP, and CI shows the highest increase in MERRA2, followed by Aqua. However, over SI, this sequence is Aqua, Terra, and MERRA2. The difference



between these two periods in the year 2020 shows a decrease except CI. Over NW, the percentage increase (decrease) in climatological (for the year 2020) AOD values were 9% (−27%), 16% (−23%), and 26% (−3%) for Terra, Aqua, and MERRA2, respectively. For EIGP, the most populated region shows the highest decrease in AOD −40%, −32%, and −22% of the pre-lockdown period, compared to an increased of 1.6%, 5.8%, and 24.5% in climatology. The same for SI regions are −13%, −7%, and −4% in the backdrop of climatological increase of 28% 31% and 22%. This decrease in the AOD over NW, EIGP, and SI is highest in Terra and least in the MERRA2. The CI region surprisingly shows an increase in AOD obtained from all the platforms. In terms of percentage for the year 2020, changes in AOD were +10%, +20%, and +18% from Terra, Aqua, and MERRA2, respectively. However, it was +11%, +14%, and +17% in the climatological average difference. The increase over CI is highest in Aqua (which is expected to see more of the anthropogenic emissions due to its later overpass time). It may be noted that the percentage contribution of natural aerosols such as dust and sea-salt in the MERRA2 data is more compared to the actual amount. Past studies have reported the overestimation of dust and sea-salt (Buchard *et al.*, 2017) and underestimation of anthropogenic aerosols (Randles *et al.*, 2016).

The ground-based AOD over six sites has also shown a significant decrease compared to the climatological difference between periods corresponding to lockdown and pre-lockdown period. The highest reduction is observed over Lahore (−60% of the pre-lockdown), followed by Kanpur (−40%). However, coastal sites such as Bhola shows the smallest decrease. Karachi, a coastal site near the Arabian Sea, shows a slight increase. The decrease in the aerosol loading is on the expected line, as the lockdown posed restriction to the transport sector, closing of shops, and limits work our of several small and big companies, hence reduces primary emissions. However, all the emissions, such as from coal-driven power plants, the energy sector, pharma industry, agriculture, and other sectors, were not entirely off and contributed to remaining aerosol, apart from natural aerosols.

Despite an overall decrease in the surface pollutant and aerosol loading over the Indian region, there is a marked increase in AOD observed over central India. CI is the second most polluted region after IGP in India (David *et al.*, 2018). Identifying the possible cause for the surprising increase in AOD forms the focus of this manuscript. Both Aqua and Terra, as well as MERRA2 reanalysis, invariably show this. However, there is no AERONET (which is only publically available ground-based observations) site over this region. Multiple factors may be responsible for this increase in aerosol loadings, such as the lenient implementation of lockdown, thereby not affecting the primary emissions. However, google mobility data shows almost a similar decrease in the percentage of mobility across all Indian states (Fig. S2). It assures that the lockdown guidelines were implemented uniformly across the country, and may not be the reason for this inadvertent increase. Other possible factors for this increase is the secondary aerosol formation due to complex chemical reactions, aerosol water, and other meteorological influences. Past studies have shown that changes in surface and upper-air circulation, wind speed, boundary layer height, and atmospheric water are closely associated with the AOD variations (Vinoj and Pandey, 2016; Srivastava, 2017; Ramachandran *et al.*, 2019). Therefore, we further examine the prevailing meteorological conditions and there changes in the next section.

3.2 Role of Meteorology

The prevailing wind pattern during the lockdown period over IGP was northwesterly, which turns to the southeasterly over southern India. Compared to climatology and pre-lockdown, there is a significant increase in wind speed over EIGP and SI. Apart from reduced emission, during this season, increased wind speed over IGP is associated with cleaner days due to enhances atmospheric dispersion capability (Vinoj and Pandey, 2016). Simultaneously over the Central Indian region where winds from northwest and southeast converge, a significant reduction was observed in wind speed. It appears CI is receiving transport from all the regions selected in our analysis (NW, EIGP, and CI) and, at the same time, experiencing a reduction in wind speed (see Fig. 3). It was hence providing a conducive environment for the stagnation of air-pollutant over this region. Day to day variation of AOD over CI is associated with the wind speed over the western part (16–22N, 72–79E) of the CI during the lockdown. Also, there is a slight increase in the fire count over the adjacent region (Fig. S3).

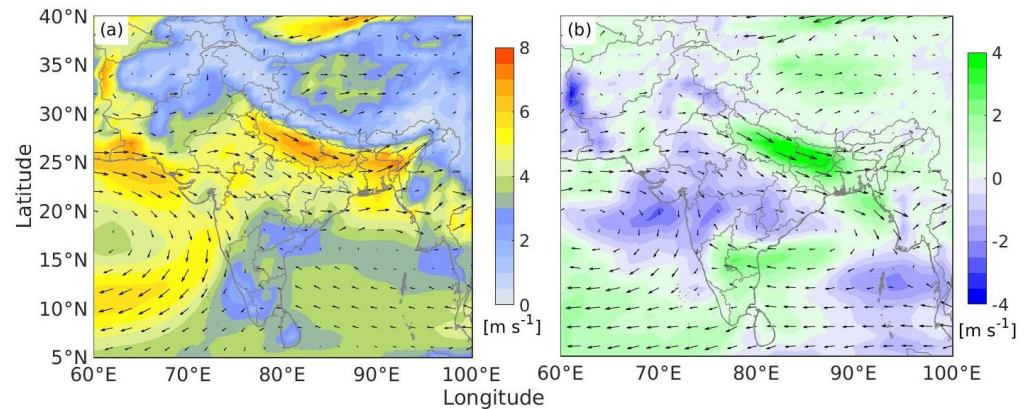
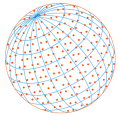


Fig. 3. (a) Climatological wind pattern (at 850 hPa) corresponding to lockdown period, shaded contour shows the wind speed (m s^{-1}) (b) Changes in the wind speed compared to climatology and pre-lockdown with overlaid wind patterns during the lockdown period.

Another important atmospheric parameter that strongly influences AOD is humidity. The pre-existing moisture was abnormally high, at the beginning of the lockdown over western CI. Both relative humidity (a measure of the degree of atmospheric saturation), and specific humidity (an indicator of the amount of actual moisture present in atmosphere) shows an increasing tendency (Figs. 4(a) and 4(b)). This increase in humidity is prominent in the mid-troposphere (700–500 hPa). Notably, the upper air RH has significantly increased (+20 in the RH unit) compared to the pre-lockdown period (Fig. 4(a)). The enhanced RH favors the aqueous chemistry, new particle formation, and deliquescence growth of existing particles, which in turn, may lead to an increase in AOD. The spatial pattern of the changes in the mean tropospheric humidity shows a substantial increase over west-central India (Fig. 4(c)). Day to day variability of the AOD, RH, wind speed also shows a concurrent variation during the lockdown period (Figs. 5(a) and 5(b)). The variation of RH and AOD is in the same phase, i.e., AOD increases with an increase in RH and reduced wind speed. Area average AOD (RH) has increased by 0.08 ± 0.01 (19.39 ± 1.48 in RH unit), which is $21 \pm 3.3\%$ ($85 \pm 6.0\%$) of the pre-lockdown period. The wind speed has reduced by $-0.48 \pm 0.15 \text{ m s}^{-1}$, which $-12 \pm 3.9\%$ of pre-lockdown values. Linear regression of AOD as a function of RH and WS shows that an increase (decrease) in RH (WS) of 20 RH unit (1 m s^{-1}) can increase AOD by 0.10 (0.04). The increase in AOD with RH is in concurrence with previous studies (Yoon and Kim, 2006; Bar-Or *et al.*, 2012; Brock *et al.*, 2016; Zang *et al.*, 2019; Eck *et al.*, 2020; Li *et al.*, 2020). The degree of change obtained using regression equation is similar to a previous study done by Yoon and Kim, 2006, an increase in RH values from 50 to 70% (in RH unit) leads to an increase in AOD at 550nm by a factor 1.24, which in the present study is 1.20. The RH can explain twenty percent of daily AOD variance (Altartatz *et al.*, 2013).

Several factors may cause an increase in AOD due to enhanced ambient moisture. For example, high humidity can increase the reaction rate of aqueous-phase oxidation of SO_2 and hence increase the sulfate aerosol (Xu *et al.*, 2019). Also, a past study has shown the rapid oxidation of SO_2 over soot particles (He and He, 2020). It is very likely possible that SO_2 emission levels may not have significantly dropped during lockdown over this region. Negligible changes were reported in the SO_2 concentration over major Indian cities (Navinya *et al.*, 2020b; Sharma *et al.*, 2020). Also, the presence of clouds in the vicinity of the aerosol layer may enhance AOD due to the hygroscopic growth, which remains valid for all aerosol types and size ranges (Eck *et al.*, 2014, 2020). Cloud can also illuminate the nearby aerosol particles, which falsely translate into AOD without an increase in actual aerosol amount.

In summary, a combination of factors appears to have increased AOD over this region. Increased mid-tropospheric RH and decreased wind speed along with residual emission, and favorable wind direction maintained high AOD during the lockdown. However, other factors such as biomass burning in the adjacent region and long-range transport of desert dust might have also contributed to this (see supplementary materials). In a recent study, Le *et al.* (2020) have also reported an interplay of atmospheric chemistry, circulation patterns, and synoptic meteorology

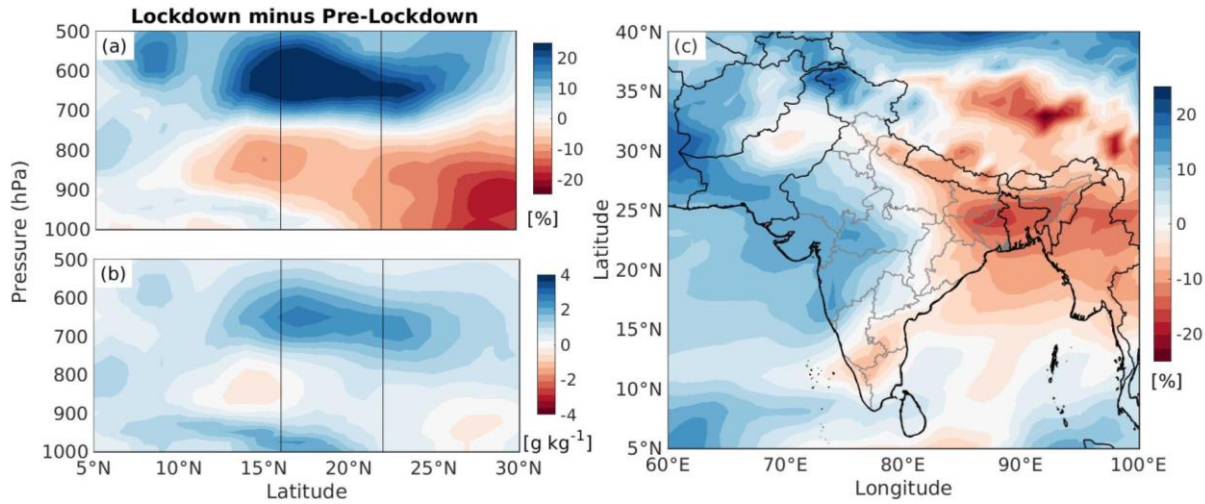
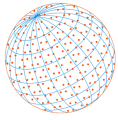


Fig. 4. Latitude-height plot of the differences (pre-lockdown minus lockdown) in (a) relative humidity and (b) specific humidity averaged over west-central India (72E–79E). Vertical lines represent the CI latitudes. (c) The spatial pattern of changes in mid-tropospheric relative humidity (700–500 hPa) during the lockdown.

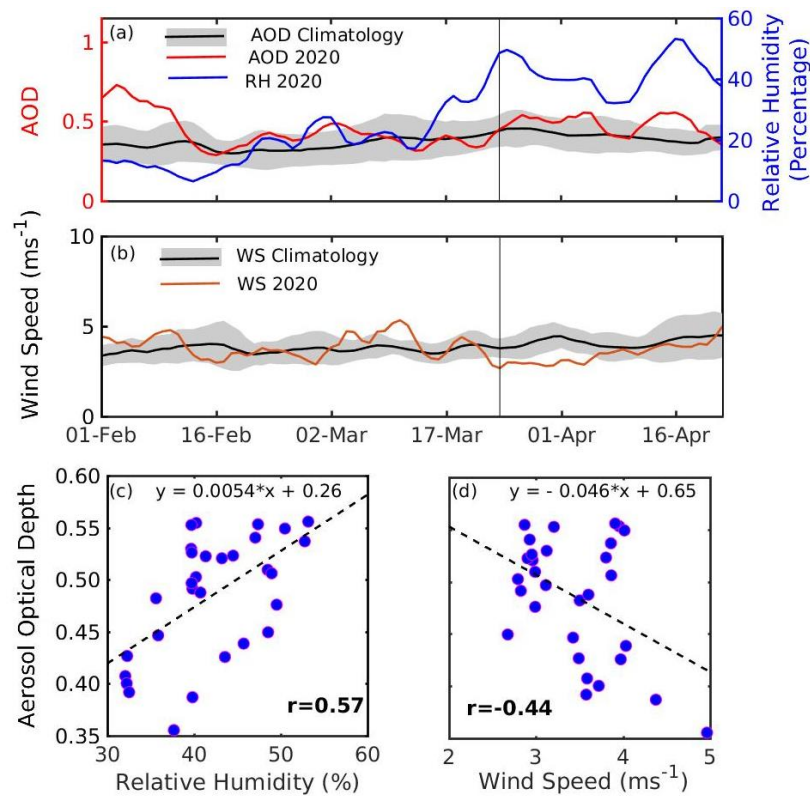
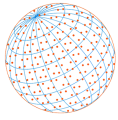


Fig. 5. Covariability of (a) AOD and mean mid-tropospheric relative humidity and (b) wind speed over Central India. The black lines (shaded region) show the intern-annual mean (standard deviation) for years 2003–2019; the vertical line shows the beginning of lockdown. Scatter plot of daily mean AOD with (c) RH and (d) wind speed during the lockdown period. Bold font for correlation coefficient (r) indicates that it is statistically significant at the 99% confidence level ($p < 0.01$).

to be responsible for an increase in the particulate pollution over Northern China during COVID19 lockdown. This study shows how changes in aerosol loading may change regional circulation and hence either amplify or suppress the initial change. Aerosol and their regional climate effects



must be understood in finer details to effectively plan for mitigation efforts to optimize air quality and climate action and their benefits.

4 SUMMARY

1. Using space-borne observations and aerosol reanalysis products, we found that a significant decline in AOD due to lockdown over the Indian region. The highest decrease was over East IGP (up to -40% of the pre-lockdown period), followed by NW (-27%) and SI (-13%). However, central India shows an increase of up to 20% .
2. Ground-based measurements also show a decrease in AOD over the Indian subcontinent. The highest decline was over Lahore (-60%), followed by Kanpur (-52.6%) and Gandhi College (-33.6%). AERONET stations at Bhola, near the Bay of Bengal coast, also show a decrease of -12% . Similarly, Karunya College, a site over southern peninsular India, shows a decrease of 28% . However, Karachi, a coastal site near the Arabian Sea, shows an increase of 4% .
3. The increase in AOD over Central India was largest from MODIS Aqua ($+20\%$), followed by MERRA2 ($+18\%$) and Terra ($+10\%$).
4. Our analysis shows that an increase in AOD of 0.08 ± 0.01 ($21 \pm 3.3\%$ of pre-lockdown period) accompanied by an increase in RH 19.39 ± 1.48 in RH unit, which is $85 \pm 6.0\%$ of the pre-lockdown period. However, the wind speed has reduced by $-0.48 \pm 0.15 \text{ m s}^{-1}$, which is $-12 \pm 3.9\%$ of pre-lockdown values.
5. Daily variability of AOD over CI was closely associated with variation of mid-tropospheric relative humidity and wind speed (850hPa) during the lockdown period. Pearson correlation coefficient of daily mean AOD with RH and wind speed 0.57 ($p = 0.001$) and -0.44 ($p = 0.01$), respectively.

ACKNOWLEDGEMENTS

The authors are grateful to the members of the NASA Goddard Space Flight Centre, who helped with the setup and the site members who helped to maintain AERONET (https://aeronet.gsfc.nasa.gov/cgi-bin/webtool_aod_v3) sites used in the present research. Data used in this study were produced with the Giovanni online data system, developed and maintained by the NASA GES DISC (<https://giovanni.gsfc.nasa.gov/giovanni/>). We acknowledge the mission scientists (MODIS) and Principal Investigators who provided the data used in this research effort. Also, ECMWF (<https://www.ecmwf.int/en/forecasts/datasets/reanalysis-datasets/era5>) and MERRA2 (<https://disc.sci.gsfc.nasa.gov/datasets?keywords=merra&page=1&project=MERRA-2>) reanalysis acknowledged for their products. IIT Bhubaneswar is acknowledged for providing the necessary infrastructure and support to carry out this research.

DISCLAIMER

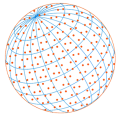
Reference to any company or specific commercial products does not constitute financial and personal conflicts of interest.

SUPPLEMENTARY MATERIAL

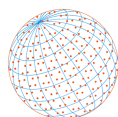
Supplementary data associated with this article can be found in the online version at <https://doi.org/10.4209/aaqr.2020.07.0466>

REFERENCES

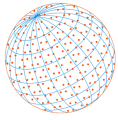
- Altaratz, O., Bar-Or, R.Z., Wollner, U., Koren, I. (2013). Relative humidity and its effect on aerosol optical depth in the vicinity of convective clouds. *Environ. Res. Lett.* 8, 034025. <https://doi.org/10.1088/1748-9326/8/3/034025>



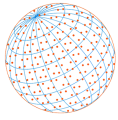
- Bao, R., Zhang, A. (2020). Does lockdown reduce air pollution? Evidence from 44 cities in northern China. *Sci. Total Environ.* 731, 139052. <https://doi.org/10.1016/j.scitotenv.2020.139052>
- Bar-Or, R.Z., Koren, I., Altaratz, O., Fredj, E. (2012). Radiative properties of humidified aerosols in cloudy environment. *Atmos. Res.* 118, 280–294. <https://doi.org/10.1016/j.atmosres.2012.07.014>
- Bauwens, M., Compornolle, S., Stavrakou, T., Müller, J.F., van Gent, J., Eskes, H., Levelt, P.F., van der A, R., Veefkind, J.P., Vlietinck, J., Yu, H., Zehner, C. (2020). Impact of Coronavirus Outbreak on NO₂ Pollution Assessed Using TROPOMI and OMI Observations. *Geophys. Res. Lett.* 47, e2020GL087978. <https://doi.org/10.1029/2020GL087978>
- Berman, J.D., Ebisu, K. (2020). Changes in U.S. air pollution during the COVID-19 pandemic. *Sci. Total Environ.* 739, 139864. <https://doi.org/10.1016/j.scitotenv.2020.139864>
- Brock, C.A., Wagner, N.L., Anderson, B.E., Beyersdorf, A., Campuzano-Jost, P., Day, D.A., Diskin, G.S., Gordon, T.D., Jimenez, J.L., Lack, D.A., Liao, J., Markovic, M.Z., Middlebrook, A.M., Perring, A.E., Richardson, M.S., Schwarz, J.P., Welti, A., Ziemba, L.D., Murphy, D.M. (2016). Aerosol optical properties in the southeastern United States in summer - Part 2: Sensitivity of aerosol optical depth to relative humidity and aerosol parameters. *Atmos. Chem. Phys.* 16, 5009–5019. <https://doi.org/10.5194/acp-16-5009-2016>
- Buchard, V., Randles, C.A., da Silva, A.M., Darmenov, A., Colarco, P.R., Govindaraju, R., Ferrare, R., Hair, J., Beyersdorf, A.J., Ziemba, L.D., Yu, H. (2017). The MERRA-2 Aerosol Reanalysis, 1980 onward. Part II: Evaluation and Case Studies. *J. Clim.* 30, 6851–6872. <https://doi.org/10.1175/JCLI-D-16-0613.1>
- Chauhan, A., Singh, R.P. (2020). Decline in PM_{2.5} concentrations over major cities around the world associated with COVID-19. *Environ. Res.* 187, 109634. <https://doi.org/10.1016/j.envres.2020.109634>
- David, L.M., Ravishankara, A.R., Kodros, J.K., Venkataraman, C., Sadavarte, P., Pierce, J.R., Chaliyakunnel, S., Millet, D.B. (2018). Aerosol optical depth over India. *J. Geophys. Res.* 123, 3688–3703. <https://doi.org/10.1002/2017JD027719>
- Dee, D.P., Uppala, S.M., Simmons, A.J., Berrisford, P., Poli, P., Kobayashi, S., Andrae, U., Balmaseda, M.A., Balsamo, G., Bauer, P., Bechtold, P., Beljaars, A.C.M., van de Berg, L., Bidlot, J., Bormann, N., Delsol, C., Dragani, R., Fuentes, M., Geer, A.J., ... Vitart, F. (2011). The ERA-Interim reanalysis: Configuration and performance of the data assimilation system. *Q. J. R. Meteorolog. Soc.* 137, 553–597. <https://doi.org/10.1002/qj.828>
- Eck, T.F., Holben, B.N., Kim, J., Beyersdorf, A.J., Choi, M., Lee, S., Koo, J.H., Giles, D.M., Schafer, J.S., Sinyuk, A., Peterson, D.A., Reid, J.S., Arola, A., Slutsker, I., Smirnov, A., Sorokin, M., Kraft, J., Crawford, J.F., Anderson, B.E., ... Park, S. (2020). Influence of cloud, fog, and high relative humidity during pollution transport events in South Korea: Aerosol properties and PM_{2.5} variability. *Atmos. Environ.* 232, 117530. <https://doi.org/10.1016/j.atmosenv.2020.117530>
- Eck, T.F., Holben, B.N., Reid, J.S., Arola, A., Ferrare, R.A., Hostetler, C.A., Crumeyrolle, S.N., Berkoff, T.A., Welton, E.J., Lolli, S., Lyapustin, A., Wang, Y., Schafer, J.S., Giles, D.M., Anderson, B.E., Thornhill, K.L., Minnis, P., Pickering, K.E., Loughner, G.P., ... Sinyuk, A. (2014). Observations of rapid aerosol optical depth enhancements in the vicinity of polluted cumulus clouds. *14*, 11633–11656. <https://doi.org/10.5194/acp-14-11633-2014>
- Filonchik, M., Hurynovich, V., Yan, H., Gusev, A., Shpilevskaya, N. (2020). Impact assessment of COVID-19 on variations of SO₂, NO₂, CO and AOD over East China. *Aerosol Air Qual. Res.* 20, 1530–1540. <https://doi.org/10.4209/aaqr.2020.05.0226>
- Gautam, S. (2020). The influence of COVID-19 on air quality in India: A boon or inutile. *Bull. Environ. Contam. Toxicol.* 104, 724–726. <https://doi.org/10.1007/s00128-020-02877-y>
- Gelaro, R., McCarty, W., Suárez, M.J., Todling, R., Molod, A., Takacs, L., Randles, C.A., Darmenov, A., Bosilovich, M.G., Reichle, R., Wargan, K., Coy, L., Cullather, R., Draper, C., Akella, S., Buchard, V., Conaty, A., da Silva, A.M., Gu, W., ... Zhao, B. (2017). The modern-era retrospective analysis for research and applications, version 2 (MERRA-2). *J. Clim.* 30, 5419–5454. <https://doi.org/10.1175/JCLI-D-16-0758.1>
- Giles, D.M., Sinyuk, A., Sorokin, M.S., Schafer, J.S., Smirnov, A., Slutsker, I., Eck, T.F., Holben, B.N., Lewis, J., Campbell, J., Welton, E.J., Korokin, S., Lyapustin, A. (2019). Advancements in the Aerosol Robotic Network (AERONET) version 3 database - automated near real-time quality control algorithm with improved cloud screening for sun photometer Aerosol Optical Depth (AOD)



- Measurements. *Atmos. Meas. Tech.* 12, 169–209. <https://doi.org/10.5194/amt-2018-272>
- He, G., He, H. (2020). Water promotes the oxidation of SO₂ by O₂ over carbonaceous aerosols. *Environ. Sci. Technol.* 54, 7070–7077. <https://doi.org/10.1021/acs.est.0c00021>
- Hersbach, H., Bell, W., Berrisford, P., Horányi, A., Sabater, J.M.S., Nicolas, J., Nicolas, M.S., Soci, C., Dee, D. (2019). Global reanalysis: goodbye ERA-Interim, hello ERA5. *ECMWF Newsl.* 159, 17–24. <https://doi.org/10.21957/vf291hehd7>
- Hsu, N.C., Jeong, M.J., Bettenhausen, C., Sayer, A.M., Hansell, R., Seftor, C.S., Huang, J., Tsay, S.C. (2013). Enhanced Deep Blue aerosol retrieval algorithm: The second generation. *J. Geophys. Res.* 118, 9296–9315. <https://doi.org/10.1002/jgrd.50712>
- Huang, C., Wang, Y., Li, X., Ren, L., Zhao, J., Hu, Y., Zhang, L., Fan, G., Xu, J., Gu, X., Cheng, Z., Yu, T., Xia, J., Wei, Y., Wu, W., Xie, X., Yin, W., Li, H., Liu, M., ... Cao, B. (2020). Clinical features of patients infected with 2019 novel coronavirus in Wuhan, China. *Lancet* 395, 497–506. [https://doi.org/10.1016/S0140-6736\(20\)30183-5](https://doi.org/10.1016/S0140-6736(20)30183-5)
- Jain, S., Sharma, T. (2020). Social and travel lockdown impact considering coronavirus disease (COVID-19) on air quality in megacities of India: Present benefits, future challenges and way forward. *Aerosol Air Qual. Res.* 20, 1222–1236. <https://doi.org/10.4209/aaqr.2020.04.0171>
- Kramer, S., Zuidema, P., Delgado, R., Silvia, A. da, Alvarez, C., Custals, L., Barkley, A., Gaston, C. J., Prospero, J.M. (2018). Comparison of saharan dust surface mass observations and lidar in Miami, FL, to the MERRA2 Reanalysis, in: AMS annual meeting 2018.
- Lal, P., Kumar, A., Kumar, S., Kumari, S., Saikia, P., Dayanandan, A., Adhikari, D., Khan, M.L. (2020). The dark cloud with a silver lining: Assessing the impact of the SARS COVID-19 pandemic on the global environment. *Sci. Total Environ.* 732, 139297. <https://doi.org/10.1016/j.scitotenv.2020.139297>
- Le Quéré, C., Jackson, R.B., Jones, M.W., Smith, A.J.P., Abernethy, S., Andrew, R.M., De-Gol, A.J., Willis, D.R., Shan, Y., Canadell, J.G., Friedlingstein, P., Creutzig, F., Peters, G.P. (2020). Temporary reduction in daily global CO₂ emissions during the COVID-19 forced confinement. *Nat. Clim. Change* 10, 647–653. <https://doi.org/10.1038/s41558-020-0797-x>
- Le, T., Wang, Y., Liu, L., Yang, J., Yung, Y.L., Li, G., Seinfeld, J.H. (2020). Unexpected air pollution with marked emission reductions during the COVID-19 outbreak in China. *Science* 7431, 702–706. <https://doi.org/10.1126/science.abb7431>
- Levy, R.C., Mattoo, S., Munchak, L.A., Remer, L.A., Sayer, A.M., Patadia, F., Hsu, N.C. (2013) The Collection 6 MODIS aerosol products over land and ocean. *Atmos. Meas. Tech.* 6, 2989–3034. <https://doi.org/10.5194/amt-6-2989-2013>
- Li, L., Li, Q., Huang, L., Wang, Q., Zhu, A., Xu, J., Liu, Z., Li, H., Shi, L., Li, R., Azari, M., Wang, Y., Zhang, X., Liu, Z., Zhu, Y., Zhang, K., Xue, S., Ooi, M.C.G., Zhang, D., Chan, A. (2020). Air quality changes during the COVID-19 lockdown over the Yangtze River Delta Region: An insight into the impact of human activity pattern changes on air pollution variation. *Sci. Total Environ.* 732, 139282. <https://doi.org/10.1016/j.scitotenv.2020.139282>
- Lokhandwala, S., Gautam, P. (2020). Indirect impact of COVID-19 on Environment: A brief study in Indian Context. *Environ. Res.* 188, 109807. <https://doi.org/10.1016/j.envres.2020.109807>
- Mahato, S., Pal, S., Ghosh, K.G. (2020). Effect of lockdown amid COVID-19 pandemic on air quality of the megacity Delhi, India. *Sci. Total Environ.* 730, 139086. <https://doi.org/10.1016/j.scitotenv.2020.139086>
- McCoy, D.T., Bender, F.A.M., Grosvenor, D.P., Mohrmann, J.K., Hartmann, D.L., Wood, R., Field, P.R. (2017). Predicting decadal trends in cloud droplet number concentration using reanalysis and satellite data. *Atmos. Chem. Phys.* 18, 2035–2047. <https://doi.org/10.5194/acp-2017-811>
- Mhawish, A., Banerjee, T., Broday, D.M., Misra, A., Tripathi, S.N. (2017). Evaluation of MODIS Collection 6 aerosol retrieval algorithms over Indo-Gangetic Plain: Implications of aerosols types and mass loading. *Remote Sens. Environ.* 201, 297–313. <https://doi.org/10.1016/j.rse.2017.09.016>
- Muhammad, S., Long, X., Salman, M. (2020). COVID-19 pandemic and environmental pollution: A blessing in disguise? *Sci. Total Environ.* 728, 138820. <https://doi.org/10.1016/j.scitotenv.2020.138820>
- Mukherjee, T., Vinoj, V. (2020). Atmospheric aerosol optical depth and its variability over an urban location in Eastern India. *Nat. Hazards.* 102, 591–605. <https://doi.org/10.1007/s11069-019-03636-x>



- Navinya, C.D., Vinoj, V., Pandey, S.K. (2020a). Evaluation of PM_{2.5} Surface Concentrations simulated by NASA's MERRA version 2 aerosol reanalysis over India and its relation to the air quality index. *Aerosol Air Qual. Res.* 20, 1329–1339. <https://doi.org/10.4209/aaqr.2019.12.0615>
- Navinya, C., Patidar, G., Phuleria, H.C. (2020b). Examining effects of the COVID-19 national lockdown on ambient air quality across urban India. *Aerosol Air Qual. Res.* 20, 1759–1771. <https://doi.org/10.4209/aaqr.2020.05.0256>
- Paital, B. (2020). Nurture to nature via COVID-19, a self-regenerating environmental strategy of environment in global context. *Sci. Total Environ.* 729, 139088. <https://doi.org/10.1016/j.scitotenv.2020.139088>
- Pandey, S.K., Bakshi, H., Vinoj, V. (2016). Recent changes in dust and its impact on aerosol trends over the Indo-Gangetic Plain (IGP). *Proc. SPIE. Remote Sens. Atmos. Clouds, Precip.* VI, 9876, 98761Z. <https://doi.org/10.1117/12.2223314>
- Pandey, S.K., Vinoj, V., Landu, K., and Babu, S.S. (2017). Declining pre-monsoon dust loading over South Asia: Signature of a changing regional climate. *Sci. Rep.* 7, 16062. <https://doi.org/10.1038/s41598-017-16338-w>
- Pandey, S.K., Vinoj, V., Panwar, A. (2020). The short-term variability of aerosols and their impact on cloud properties and radiative effect over the Indo-Gangetic Plain. *Atmos. Pollut. Res.* 11, 630–638. <https://doi.org/10.1016/j.apr.2019.12.017>
- Ramachandran, S., Rajesh, T.A., Kedia, S. (2019). Influence of relative humidity, mixed-layer height, and mesoscale vertical-velocity variations on column and surface aerosol characteristics over an urban region. *Boundary Layer Meteorol.* 170, 161–181. <https://doi.org/10.1007/s10546-018-0384-0>
- Randles, C.A., da Silva, A.M., Buchard, V., Colarco, P.R., Darmenov, A., Govindraju, R., Smirnov, A., Holben, B., Ferrare, R., Hair, J., Shinzuka, Y., Flynn, C.J. (2017). The MERRA-2 Aerosol reanalysis, 1980 onward. part i: system description and data assimilation evaluation. *J. Clim.* 30, 6823–6850. <https://doi.org/10.1175/JCLI-D-16-0609.1>
- Randles, C.A., da Silva, A.M., Buchard, V., Darmenov, A., Colarco, P.R., Aquila, V., Bian, H., Nowottnick, E.P., Pan, X., Smirnov, A., Yu, H. (2016). The MERRA-2 aerosol assimilation. *NASA Tech. Rep. Series on Global Modeling and Data Assimilation*, 45.
- Satheesh, S.K., Ramanathan, V. (2000). Large differences in tropical aerosol forcing at the top of the atmosphere and Earth's surface. *Nature* 405, 60–63. <https://doi.org/10.1038/35011039>
- Sharma, S., Zhang, M., Anshika., Gao, J., Zhang, H., Kota, S.H. (2020). Effect of restricted emissions during COVID-19 on air quality in India. *Sci. Total Environ.* 72, 1315. <https://doi.org/10.1016/j.scitotenv.2020.138878>
- Shi, X., Brasseur, G.P. (2020). The response in air quality to the reduction of Chinese economic activities during the COVID-19 outbreak. *Geophys. Res. Lett.* 47, e2020GL088070. <https://doi.org/10.1029/2020GL088070>
- Sicard, P., De Marco, A., Agathokleous, E., Feng, Z., Xu, X., Paoletti, E., Rodriguez, J.J.D., Calatayud, V. (2020). Amplified ozone pollution in cities during the COVID-19 lockdown. *Sci. Total Environ.* 735, 139542. <https://doi.org/10.1016/j.scitotenv.2020.139542>
- Sinyuk, A., Holben, B.N., Eck, T.F., Giles, D.M., Slutsker, I., Korokin, S., Schafer, J.S., Smirnov, A., Sorokin, N., Lyapustin, A. (2020). The AERONET Version 3 aerosol retrieval algorithm, associated uncertainties and comparisons to Version 2. *Atmos. Meas. Tech.* 13, 3375–3411. <https://doi.org/10.5194/amt-13-3375-2020>
- Srivastava, R. (2017). Trends in aerosol optical properties over South Asia. *Int. J. Climatol.* 37, 371–380. <https://doi.org/10.1002/joc.4710>
- Tiwari, S., Dumka, U.C., Kaskaoutis, D.G., Ram, K., Panicker, A.S., Srivastava, M.K., Tiwari, S., Attri, S.D., Soni, V.F., Pandey, A.K. (2016). Aerosol chemical characterization and role of carbonaceous aerosol on radiative effect over Varanasi in central Indo-Gangetic Plain. *Atmos. Environ.* 125, 437–449. <https://doi.org/10.1016/j.atmosenv.2015.07.031>
- Vinoj, V., Satheesh, S.K. (2004). Direct and indirect radiative effects of sea-salt aerosols over Arabian Sea. *Curr. Sci.* 86, 1381–1390. <http://www.jstor.org/stable/24109210>
- Vinoj, V., Satheesh, S.K., Moorthy, K.K. (2010). Optical, radiative, and source characteristics of aerosols at Minicoy, a remote island in the southern Arabian Sea. *J. Geophys. Res.* 115, D01201. <https://doi.org/10.1029/2009JD011810>
- Vinoj, V., Pandey, S.K. (2016). Towards understanding the variability of aerosol characteristics



- over the Indo-Gangetic Plain. *Remote Sens. Model. Atmos. Ocean. Interact.* 9882, 988205. <https://doi.org/10.1117/12.2223315>
- Wang, Q., Su, M. (2020). A preliminary assessment of the impact of COVID-19 on environment – A case study of China. *Sci. Total Environ.* 728, 138915. <https://doi.org/10.1016/j.scitotenv.2020.138915>
- Wei, J., Li, Z., Peng, Y., Sun, L. (2019a). MODIS Collection 6.1 aerosol optical depth products over land and ocean: Validation and comparison. *Atmos. Environ.* 201, 428–440. <https://doi.org/10.1016/j.atmosenv.2018.12.004>
- Wei, J., Li, Z., Sun, L., Peng, Y., Wang, L. (2019b). Improved merge schemes for MODIS Collection 6.1 Dark Target and Deep Blue combined aerosol products. *Atmos. Environ.* 202, 315–327. <https://doi.org/10.1016/j.atmosenv.2019.01.016>
- World Health Organization (WHO) (2020). Coronavirus Disease 2019: Situation report-158. https://www.who.int/docs/default-source/coronaviruse/situation-reports/20200626-covid-19-sitrep-158.pdf?sfvrsn=1d1aae8a_2
- Xu, J., Zhu, F., Wang, S., Zhao, X., Zhang, M., Ge, X., Wang, J., Tian, W., Wang, L., Yang, L., Ding, L., Lu, X., Chen, X., Zheng, Y., Guo, Z. (2019). Impacts of relative humidity on fine aerosol properties via environmental wind tunnel experiments. *Atmos. Environ.* 206, 21–29. <https://doi.org/10.1016/j.atmosenv.2019.03.002>
- Yang, L., Mukherjee, S., Pandithurai, G., Waghmare, V., Safai, P.D. (2019). Influence of dust and sea-salt sandwich effect on precipitation chemistry over the Western Ghats during summer monsoon. *Sci. Rep.* 9, 1–13. <https://doi.org/10.1038/s41598-019-55245-0>
- Yoon, S.C., Kim, J. (2006). Influences of relative humidity on aerosol optical properties and aerosol radiative forcing during ACE-Asia. *Atmos. Environ.* 40, 4328–4338. <https://doi.org/10.1016/j.atmosenv.2006.03.036>
- Yunus, A.P., Masago, Y., Hijioka, Y. (2020). COVID-19 and surface water quality: Improved lake water quality during the lockdown. *Sci. Total Environ.* 731, 139012. <https://doi.org/10.1016/j.scitotenv.2020.139012>
- Zambrano-Monserrate, M.A., Ruano, M.A., Sanchez-Alcalde, L. (2020). Indirect effects of COVID-19 on the environment. *Sci. Total Environ.* 728, 138813. <https://doi.org/10.1016/j.scitotenv.2020.138813>
- Zang, L., Wang, Z., Zhu, B., Zhang, Y. (2019). Roles of relative humidity in aerosol pollution aggravation over central China during wintertime. *Int. J. Environ. Res. Public Health.* 16, 4422. <https://doi.org/10.3390/ijerph16224422>
- Zhou, P., Yang, X.L., Wang, X.G., Hu, B., Zhang, L., Zhang, W., Si, H.R., Zhu, Y., Li, B., Huang, C.L., Chen, H.D., Chen, J., Luo, Y., Guo, H., Jiang, R.D., Liu, M.Q., Chen, Y., Shen, X.R., Wang, X., ... Shi, Z.I. (2020). A pneumonia outbreak associated with a new coronavirus of probable bat origin. *Nature* 579, 270–273. <https://doi.org/10.1038/s41586-020-2012-7>